JOURNAL OF GEOPHYSICAL RESEARCH, VOL. 115, C04026, doi:10.1029/2009JC005853, 2010

Wave-turbulence interaction and its induced mixing in the upper ocean

Chuan Jiang Huang[1] and Fangli Qiao[1]

Received 26 September 2009; revised 1 December 2009; accepted 15 December 2009; published 30 April 2010.

[1] In the ocean, interaction among the mean current, the surface waves, and turbulence is a major mechanism for energy transfer from surface waves to the turbulence field. This process is associated with attenuation of surface waves. This paper deals with wave-turbulence interaction and its induced mixing using field observations and a one-dimensional, level 2.5 turbulence closure model. The results show that both the turbulence kinetic energy dissipation rate and the vertical mixing induced by wave-turbulence interaction are a function of $u_{s0}u_*^2$ and wave parameters, where u_{s0} is the Stokes drift at the sea surface and u_* is the friction velocity in water. The former decays with the depth away from the surface in the form of e^{2kz}, while the latter decays as e^{3kz} (k is the wave number). We also analyze the wave decay induced by wave-turbulence interaction. The decay time scale is in proportion to cL/u_*^2, while in inverse proportion to $\sqrt{\delta}$, where c is a phase speed, L is a wavelength, and δ is a wave steepness. A series of numerical experiments are performed to evaluate the effects of wave-turbulence interaction. The results from the cases with effects of wave-turbulence interaction show significant improvement in simulation of turbulence characteristics compared to the cases in the absence of surface waves. This implies that wave-turbulence interaction is a significant mechanism for generation of turbulence kinetic energy in the upper ocean and plays an important role in regulating vertical mixing and surface wave decay.

Citation: Huang, C. J., and F. Qiao (2010), Wave-turbulence interaction and its induced mixing in the upper ocean, *J. Geophys. Res.*, *115*, C04026, doi:10.1029/2009JC005853.

1. Introduction

[2] Surface waves are a kind of the most important dynamical processes in the ocean because of their strong influences on exchanges of the momentum, heat, and mass between the ocean and atmosphere. Wind energy input to surface waves was estimated as 60~70 TW [*Wang and Huang*, 2004; *Rascle et al.*, 2008] with a seasonal variation of 43–82 TW [*Teng et al.*, 2009]. These values are much larger than the mechanical energy from all other sources in the ocean [*Ferrari and Wunsch*, 2009].

[3] In the past several decades, efforts have focused on the effects of wave breaking on the upper ocean [*Agrawal et al.*, 1992; *Craig and Banner*, 1994; *Terray et al.*, 1996]. Most of wave energy is dissipated locally through wave breaking [*Donelan*, 1998], which greatly enhances turbulence kinetic energy (hereafter TKE) near the sea surface [*Agrawal et al.*, 1992; *Drennan et al.*, 1996]. Maximum values of enhancement are up to 200 times of the wall layer value [*Young and Babanin*, 2006]. However, the strong turbulence induced by wave breaking is mainly confined within the near-surface zone with the depth scale of wave height [*Rapp and Melville*, 1990; *Craig and Banner*, 1994; *Soloviev and Lukas*, 2003]. Thus, it is controversial about the effects of wave breaking on the upper ocean [e.g., *Burchard*, 2001; *Mellor and Blumberg*, 2004; *Zhang et al.*, 2007].

[4] Besides above mentioned wave breaking, interaction among the mean current, the surface waves, and turbulence also plays an important role in the budget of TKE of the upper ocean. It is believed that in the real ocean the surface waves are not truly irrotational or potential before breaking [*Phillips*, 1961]. The surface waves, the mean current, and turbulence can interact in a variety of ways. Meanwhile, the wave energy can transfer to the turbulence field associated with attenuation of surface waves. This phenomenon has repetitiously been confirmed by theoretical analyses [*Phillips*, 1961; *Kitaigorodskii et al.*, 1983; *Ardhuin and Jenkins*, 2006], laboratory experiments [*Cheung and Street*, 1988; *Teixeira and Belcher*, 2002; *Babanin and Haus*, 2009; D. J. Dai et al., An experiment on the non-breaking surface wave–induced vertical mixing, submitted to *Journal of Physical Oceanography*, 2009], and field observations [*Anis and Moum*, 1995; *Gemmrich and Farmer*, 2004; *Veron et al.*, 2009].

[5] Laboratory experiments by *Cheung and Street* [1988] indicated that interaction among the mean current, waves and turbulence fields always occurs in the wind-ruffled mechanically generated wave cases. It is the interaction to cause kinetic energy transfer from the wavefield to the mean

[1]Key Laboratory of Marine Science and Numerical Modeling, First Institute of Oceanography, State Oceanic Administration, Qingdao, China.

0148-0227/10/2009JC005853

current by the wave-induced Reynolds stress, and in turn transfer to turbulence by the turbulence viscosity. *Thais and Magnaudet* [1996] also pointed out that the structure of the turbulent field below surface waves is different from that near a wall. Subsequently, these results were confirmed by field experiments [*Anis and Moum*, 1995], which showed similar wave-turbulence interaction in the real ocean when the swells were present. Based on dissipation measurements from a surface-following float in the open ocean, *Gemmrich and Farmer* [2004] analyzed the turbulence structure beneath breaking and nonbreaking waves, and found that the occurrence and magnitude of the prebreaking turbulence are consistent with that induced by wave-turbulence interaction in a rotational wavefield. Recently, laboratory experiments by *Babanin and Haus* [2009] and Dai et al. (submitted manuscript, 2009) further revealed the existence of turbulence induced by nonbreaking surface waves.

[6] *Jiang et al.* [1990] argued that wave-turbulence interaction can result in significant energy transfer among the mean, waves, and turbulence fields, although the momentum transfer is not significant. The TKE induced by wave-turbulence interaction can regulate the vertical mixing, then affect the upper ocean. *Jacobs* [1978] suggested that the effects of the mixing induced by surface waves are important for accurate temperature predictions in the upper ocean. From the Reynolds stress expression, *Qiao et al.* [2004] derived a parameterization scheme of nonbreaking wave induced mixing based on the wave number spectrum. This scheme has been incorporated into ocean and coastal circulation models [e.g., *Qiao et al.*, 2004; *Xia et al.*, 2006], as well as climate models [*Song et al.*, 2007; *Huang et al.*, 2008]. All numerical experiments show that incorporation of the waves into the models leads significant improvement in simulation of the upper ocean temperature structure.

[7] This paper will examine wave-turbulence interaction in the ocean and develop a wave-turbulence interaction induced mixing scheme. The TKE dissipation rate induced by wave-turbulence interaction is addressed in section 2. Its induced vertical mixing and surface wave decay are discussed in sections 3 and 4. The results are confirmed using a one-dimensional turbulence closure model in section 5. Section 6 includes conclusion remarks.

2. TKE Dissipation Rate

[8] Wave-turbulence interaction in the ocean is related to the complicated coupling among the mean current, wave motion, and turbulence. However, understanding of dynamical processes involved remains rudimentary, though great efforts have been devoted during the past several decades. *Kitaigorodskii and Lumley* [1983] argued that the primary effect of wave-turbulence interaction is the transport of wave energy away from the surface by turbulence. *Cheung and Street* [1988] and *Thais and Magnaudet* [1996] suggested that wave-turbulence interaction is resulted from the wave-induced stress, because the wave motion does not remain truly irrotational. Besides the wave stress, *Anis and Moum* [1995] suggested that the downward transport of TKE by the wave motion is also a possible mechanism for wave-turbulence interaction. In other studies, such as *Teixeira and Belcher* [2002] and *Ardhuin and Jenkins* [2006], wave-turbulence interaction was attributed to the distortion of turbulence by the Stokes drift. In addition, the previous investigators found that the Langmuir circulation, which arises through the interaction of vorticity and the Stokes drift induced by surface waves, also belongs to the motions induced by wave-turbulence interaction, which transfers the wave energy to the turbulence [*McWilliams et al.*, 1997; *Plueddemann et al.*, 1996; *Veron et al.*, 2009].

[9] According to the previous investigations, such as *McWilliams et al.* [1997], *Teixeira and Belcher* [2002], *Kantha and Clayson* [2004], and *Ardhuin and Jenkins* [2006], the TKE dissipation rate ε_w induced by wave-turbulence interaction can be expressed as

$$\varepsilon_w = -\overline{u'w'}\frac{\partial u_s}{\partial z}, \tag{1}$$

where u' and w' are horizontal and vertical velocity fluctuations, respectively, and z is the vertical coordinate with an origin at the mean sea level and positive upward. In the upper ocean, $-\overline{u'w'} \sim u_*^2$, in which $u_* = \sqrt{\tau_0/\rho}$ is the friction velocity in water, τ_0 is the surface wind stress, and ρ is the density of the seawater [*Mellor and Yamada*, 1982; *Lettvin and Vesecky*, 2001]. The Stokes drift induced by surface waves can be expressed as

$$u_s = u_{s0}e^{2kz}, \tag{2}$$

where u_{s0} ($= c(Ak)^2$) is the magnitude of the Stokes drift at the surface ($z = 0$), c is the phase speed, A ($= H_s/2$) is the wave amplitude, H_s is the significant wave height, k ($= 2\pi/L$) is the wave number, and L is the wavelength. Thus ε_w can be written as

$$\varepsilon_w = a_1 u_*^2 \frac{\partial u_s}{\partial z} = 4\pi a_1 \frac{u_{s0}u_*^2}{L}e^{2kz}, \tag{3}$$

where the a_1 is a dimensionless constant associated with characteristics of surface waves, which can be determined by regression of the observational data.

[10] *Anis and Moum* [1995] analyzed two experiments conducted off the Oregon coast in the summer 1989 and 1990 (OR89 and OR90, hereafter). OR90 was carried out two daytimes and three nighttimes (OR90d1, OR90d2, OR90n1, OR90n2, and OR90n3, hereafter). During the experiments, the microscale structures of the temperature, conductivity, and velocity shear were collected using a microstructure profiler. (OR89 was carried through two nighttimes, for OR89n1 and OR89n2, hereafter, the salinity was not measured). From the data, the profiles of potential density σ_θ and the TKE dissipation rate ε were calculated (in Figure 1 of *Anis and Moum* [1995]). On the other hand, they estimated the significant wave height H_s, and periods T of the swells and wind waves, as well as the surface wind stress τ_0 (see Table 1). These experiments were conducted in water depths between 1000 and 2000 m, thus other characteristics of waves can approximately be estimated from the classical relations of the linear monochromatic deep water wave if needed.

[11] According to OR89 and OR90, the value of a_1 in equation (3) can be set as

$$a_1 = 3.75\beta\pi\sqrt{\frac{H_s}{L}} = 3.75\beta\pi\sqrt{\delta}, \tag{4}$$

Table 1. Parameters of the Swells and Sea State Conditions for OR90 and OR89[a]

	Experiment						
	OR90d1	OR90d2	OR90n1	OR90n2	OR90n3	OR89n1	OR89n2
τ_0 (N m^{-2})	0.05	0.14	0.23	0.12	0.03	0.25	0.11
H_s (m)	1.2	1.8	2.0	1.8	1.8	3.0 2.5	2.0
T (s)	6	6	5	6	7	12 6	8

[a]Taken from *Anis and Moum* [1995, Table 1]. τ_0 is the local surface wind stress. H_s and T are the significant wave height and wave period, respectively. *Anis and Moum* [1995] cannot give the period T of the swell in OR90d1, so we set it to 6 s according to other observations. These experiments were conducted in water depths between 1000 and 2000 m, thus other characteristics of waves were obtained from the following formula: the wave amplitude $A = H_s/2$, the phase speed $c = gT/2\pi$, the wavelength $L = gT^2/2\pi$, and the wave number $k = 2\pi/L$.

where β is a dimensionless constant, which is equal to or less than 1.0, and $\delta = H_s/L$ is the wave steepness. Combining equations (3) and (4), yields

$$\varepsilon_w = 15\beta\pi^2\sqrt{\delta}\frac{u_{s0}u_*^2}{L}e^{2kz} = 148\beta\sqrt{\delta}\frac{u_{s0}u_*^2}{L}e^{2kz}. \quad (5)$$

From equation (5), the magnitude of the dissipation rate ε_w induced by wave-turbulence interaction is in proportion to $u_{s0}u_*^2$, here $u_{s0}u_*^2$ can be written as $u_{s0}\tau_0/\rho$, which is in proportion to the Stokes dissipation rate of surface waves [*Kantha et al.*, 2009]. The Stokes dissipation of surface waves is very strong in the ocean. It was estimated as 2.5 TW by *Kantha et al.* [2009], while it was estimated as 6 TW by *Rascle et al.* [2008] in the global ocean. On the other hand, the dissipation rate ε_w has a scale of $\sqrt{\delta}/L$ (or $H_s^{1/2}L^{-3/2}$). This implies that the waves with larger amplitudes or shorter wavelengths would induce stronger dissipation in the ocean. However, this dissipation rate decays downward as e^{2kz} away from the surface, which is similar to that from the wave stresses by *Anis and Moum* [1995], as well as that from the viscosity effect by *Phillips* [1961] and *Kinsman* [1965]. The previous investigations indicated that the dissipation induced by short waves attenuates rapidly with the depth due to their large wave number, so that the wave effects are confined within a thin layer near the surface, whereas that induced by the swells with small wave number would penetrate a great depth, and then it may play an important role in regulating the upper ocean mixing and the stratification.

[12] Figure 1 shows a comparison of the dissipation rate ε_w induced by wave-turbulence interaction with the observations in OR90. The values of β are shown in Table 2. The wind wave effect is smaller than that of the swells because of their small wave heights in OR89 and OR90 (Figures 1b–1d), so that it can be neglected. In OR90d1 and OR90n3, the surface wind stress and heat flux are very small, and no discernible whitecaps were present, therefore, the dissipation rate in the upper ocean may mainly be controlled by wave-turbulence interaction, and ε_w predicted by equation (5) is very close to the observations (Figures 1a and 1e). In other three experiments, there are biases between the predicted turbulence rates and the observations (Figures 1b–1d), implying that other processes, such as wave breaking, the mean current shear, and the buoyancy, may also play a role in regulating the TKE in the upper ocean.

[13] Similar to Figure 1, Figure 2 shows a comparison of the dissipation rate ε_w with the observations in OR89. There were two swell systems in OR89n1, one with a period of about 12 s and a significant wave height of 3.0 m, and another with a period of 6 s and a wave height of 2.5 m (Table 1). The observed dissipation rate is in good agreement with that predicted from the two swell systems with the depth deeper than 6 m; whereas it is much larger than that estimated from swells within the upper 6 m (Figure 2a), implying a possible link to wave breaking.

[14] The effect of wave-turbulence interaction is further evaluated by the observations by *Wüest et al.* [2000] (Figure 3) and *Osborn et al.* [1992] (Figure 4). The observations by *Wüest et al.* [2000] were conducted in a medium-scale

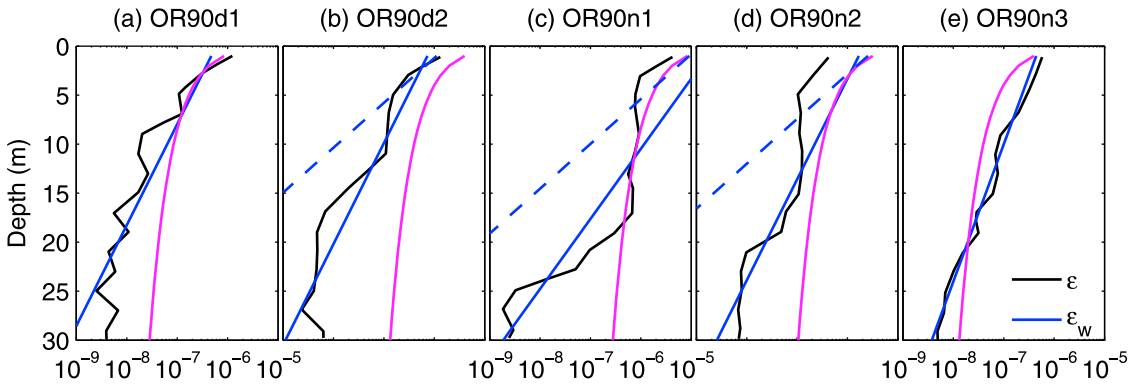

Figure 1. Comparisons of the dissipation rates by the swells (ε_w, blue lines) with the observations (ε, black lines) in OR90 (in m^2 s^{-3}). The pink lines represent the dissipation rates predicted by the law of the wall, and the blue dashed lines are those predicted by wind waves (with a wave period of 4 s and wave height of 0.9 m). The values of β in equation (5) are listed in Table 2.

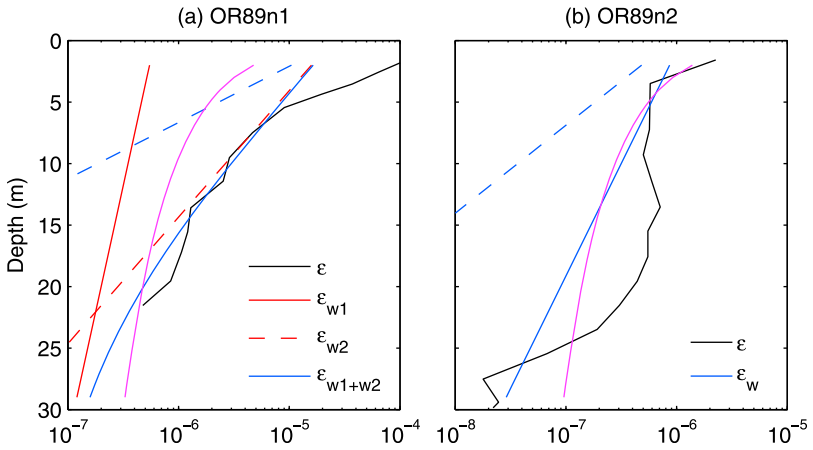

Figure 2. Similar to Figure 1 but for OR89 (in $m^2\ s^{-3}$). There were two swell systems for OR89n1: the red line represents the case with $T = 12$ s and $H_s = 3.0$ m, the red dashed line represents the case with $T = 6$ s and $H_s = 2.5$ m, and the blue line is their sum. The values of β in equation (5) are listed in Table 2.

lake. In Figure 3, the friction velocity is 3.1×10^{-3} m s^{-1} (in Table 1 of *Wüest et al.* [2000]), and the period and amplitude of waves are assumed to be 4 s and 0.25 m.

[15] For observation by *Osborn et al.* [1992], both the waves and swells appeared, but the wave heights and periods of swells were not measured, thus we took the effect of the dominant waves with period of 4 s and amplitude of 0.28 m into account only (in the appendix of *Osborn et al.* [1992]). For the observation, there also was obvious wave breaking, so that the observed dissipation rates near the surface are significantly greater than predicted (Figure 4). In addition, it is worth noting that near the surface the magnitude of the dissipation rate predicted by equation (5) is close to that by the law of the wall, while the former attenuates more rapidly with the depth than the latter.

3. Wave-Induced Mixing

[16] It is believed that as a kind of small-scale processes, the surface waves affect the ocean and climate system mainly through regulating the vertical mixing in the upper ocean. Following the Prandtl mixing length theory, the mixing induced by wave-turbulence interaction can be written as [*Jacobs*, 1978]

$$B_v = l_w^2 S_w, \tag{6}$$

where S_w is associated with the vertical shear of surface wave orbital velocity, and the mixing length l_w is proportional to the wave particle displacement [*Jacobs*, 1978; *Qiao et al.*, 2004; *Babanin*, 2006; *Babanin and Haus*, 2009], i.e.,

$$S_w = a_2 A c k^2 e^{kz} = a_2 \frac{u_{s0}}{A} e^{kz}, \tag{7}$$

and

$$l_w = a_3 A e^{kz}. \tag{8}$$

Thus,

$$B_v = \alpha A u_{s0} e^{3kz}, \tag{9}$$

where α ($= a_2 a_3^2$) is a dimensionless constant, which is determined by the characteristics of surface waves. Fitting the observations in OR90, yields,

$$\alpha = 10^5 \frac{2u_*^2}{gL}, \tag{10}$$

where g is the gravitational acceleration. Then, we have

$$B_v = 10^5 \delta \frac{u_{s0} u_*^2}{g} e^{3kz}. \tag{11}$$

On the other hand, the vertical mixing can be obtained from the Osborn dissipation model in the stratified ocean [*Osborn*, 1980], in which the mixing K_h is directly related to the dissipation rate ε and the buoyancy frequency N ($= \sqrt{-\frac{g}{\rho_0}\frac{\partial \sigma_\theta}{\partial z}}$), i.e.,

$$K_h = \Gamma \frac{\varepsilon}{N^2}, \tag{12}$$

where Γ is the so-called mixing efficiency dependent on a flux Richardson number, which is set as 0.2 in the following discussion.

[17] The square of the buoyancy frequency N^2 in OR90 is shown in Figure 5. Figure 6 compares B_v induced by wave-

Table 2. Parameter β in Equation (5), the Decay Time T_d, and the Decay Length L_d of Swells in OR90 and OR89

	Experiment						
	OR90d1	OR90d2	OR90n1	OR90n2	OR90n3	OR89n1	OR89n2
β	0.75	0.15	0.75	0.40	1.00	1.00, 1.00	1.00
T_d (days)	11.8	18.6	1.0	8.2	24.2	19.4, 1.3	10.7
L_d (× 100 km)	47.9	75.4	3.5	33.0	114.0	156.9, 5.4	57.5

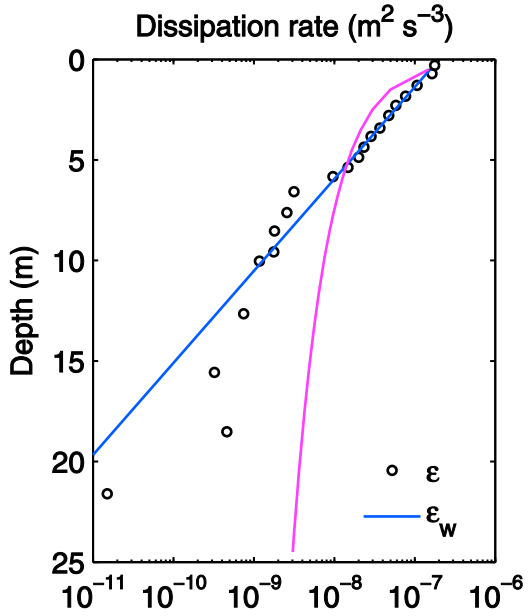

Figure 3. Comparisons of the dissipation rates by the waves (ε_w, blue lines) with data from *Wüest et al.* [2000, Figure 4] (ε, hollow circles) (in m^2 s^{-3}). The pink lines represent the dissipation rates predicted by the law of the wall. The friction velocity is 3.1×10^{-3} m s^{-1} (in Table 1 of *Wüest et al.* [2000]), and the period and amplitude of waves are assumed to be 4 s and 0.25 m, respectively. Parameter β in equation (5) is set as 1.0.

turbulence interaction with that from the Osborn dissipation model. One can see that B_v is in good agreement with K_h in most observations, implying that the vertical mixing in the upper ocean may be controlled by wave-turbulence interaction in these cases. Similar to the dissipation rate, B_v induced by the wind waves is far smaller than that by the swells due to their small amplitudes (Figures 6b–6d), so that their effects are neglected in these cases.

[18] Equation (11) indicates that the strength of B_v depends on combined effects of the Stokes drift, local wind stress ($u_*^2 = \tau_0/\rho$), and wave steepness, thus the larger wind stress and steeper waves would result in a larger B_v. On the other hand, since B_v decays downward as e^{3kz} away from the surface, and seems independent of stratification, the effect of B_v can extend to tens of meters for the swells with small wave numbers, which is much deeper than that achieved by wave breaking.

[19] The mixed layer is very shallow at middle and high latitudes in summer due to the strong solar radiation. The minimal mixed layer depth is only about 10 m [*Kara et al.*, 2003]. Thus B_v could penetrate through the mixed layer and reach the subsurface, thus affect stratification in the upper ocean.

4. Decay of Swells

[20] Wave-turbulence interaction extracts the energy from surface waves, and results in the wave decay. It is believed that long-period swells can propagate over a long distance with a little energy loss, while short-period and steep swells are attenuated in a matter of days [*Kantha*, 2006; *Ardhuin and Jenkins*, 2006].

[21] The decay of wave energy caused by wave-turbulence interaction can be expressed as

$$\frac{\partial E_w}{\partial t} = -\int_{-\infty}^{0} \rho \varepsilon_w dz. \tag{13}$$

Similar to *Kantha* [2006], we define a decay time scale T_d of waves as that for the wave amplitude to decrease by 50%. For the deep ocean, the energy of surface waves $E_w = \rho g A^2/2$, and the group speed $c_g = c/2$. Integrating equation (13), yields

$$T_d = \frac{cL}{89\beta\sqrt{\delta}u_*^2}, \tag{14}$$

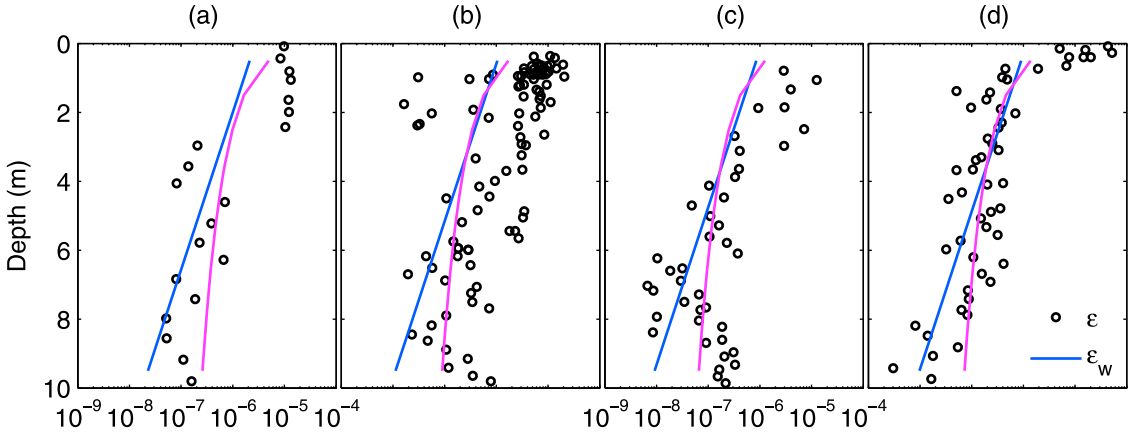

Figure 4. Comparisons of the dissipation rates by wind waves (ε_w, blue lines) with data from *Osborn et al.* [1992, Figures 9a–9d] (ε, hollow circles) (in m^2 s^{-3}). The pink lines represent the dissipation rates predicted by the law of the wall. Wind stress data are taken from Table 1 of *Osborn et al.* [1992]. In all cases, the period and amplitude of waves are set as 4 s and 0.28 m, respectively. Parameter β in equation (5) is set as 1.0.

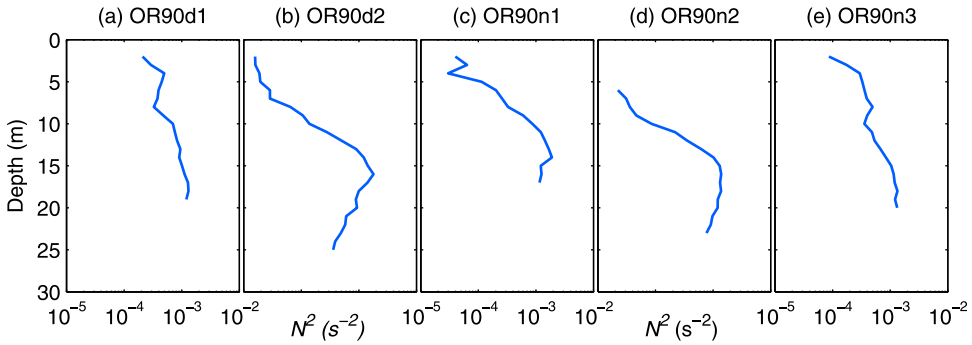

Figure 5. The square of the buoyancy frequency N^2 for OR90 (in s^{-2}).

and the decay length

$$L_d = c_g T_d = \frac{c^2 L}{178\beta\sqrt{\delta}u_*^2}. \tag{15}$$

In equation (14), the decay time T_d is in proportion to cL/u_*^2, which is similar to pervious studies, such as *Teixeira and Belcher* [2002], *Kantha* [2006], and *Ardhuin and Jenkins* [2006]. However, T_d here is in inverse proportion to the square root of the wave steepness, implying that the decay time is much longer for the smooth waves.

[22] Table 2 lists the decay time scale T_d and decay length L_d of the swells in the cases of OR90 and OR89. One can see that the decay times varied from about 1.0 to 24.2 days, and decay lengths from 350 to 15,690 km. These estimated values are very sensitive to the swell period. For OR89n1, for the swell with a period of 12s, the decay time and length were 19.4 days and 15,690 km, respectively, while they were only 1.3 days and 540 km for that with a period of 6s. Note that, T_d and L_d depend on the local wind stress. For OR90d1 with a surface wind stress of 0.05 N m^{-2}, the swells had a period of 6 s, the decay time and length were 11.8 days and 4790 km, which were much larger than that for OR89n1. We compare the decay coefficients for these cases, and note that the decay time scale estimated by equation (14) is smaller than that by *Kantha* [2006] and *Ardhuin and Jenkins* [2006], when β is set as 1.0, but larger than that by *Teixeira and Belcher* [2002].

[23] It should be noted that other mechanisms besides wave-turbulence interaction can also extract the energy from the swells. For example, the swells would interact with the atmosphere and lose their momentum and energy to the surface winds during propagating over the ocean [*Grachev and Fairall*, 2001; *Kudryavtsev and Makin*, 2004]. Thus the real dissipation rate of swells is larger than that expected by equation (5), and the decay time and length scales should be smaller than that predicted by equations (14) and (15).

5. Confirmation by Numerical Modeling

5.1. Model Linkage

[24] A one-dimensional, level 2.5 version Mellor-Yamada [*Mellor and Yamada*, 1982] turbulence closure model is employed to examine the effects of wave-turbulence interaction on the upper ocean mixing in this section. This model is the same as that used by *Mellor and Blumberg* [2004], in which the vertical viscosity K_m and diffusivity K_h are defined as

$$K_m = qlS_m, \tag{16a}$$

and

$$K_h = qlS_h, \tag{16b}$$

where $q^2/2$ is TKE, l is a turbulence length scale, and S_m and S_h are stability functions associated with the

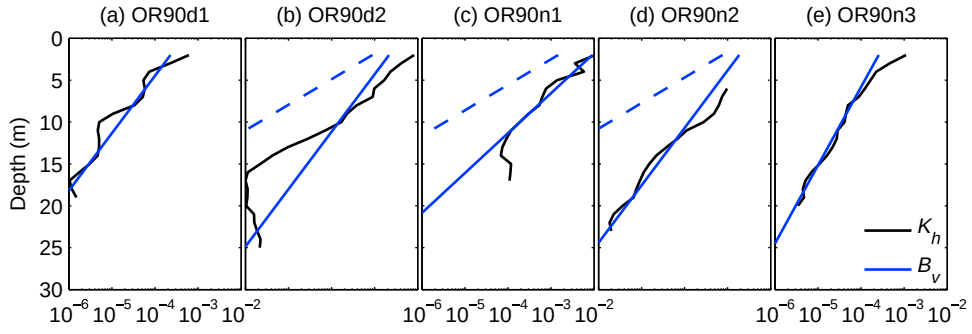

Figure 6. Comparisons of the vertical mixing B_v by the swells (blue lines) and that from the Osborn dissipation model K_h (black lines) for OR90 (in m^2 s^{-1}). The blue dashed lines represent B_v induced by wind waves (with the wave period of 4 s and wave height of 0.9 m).

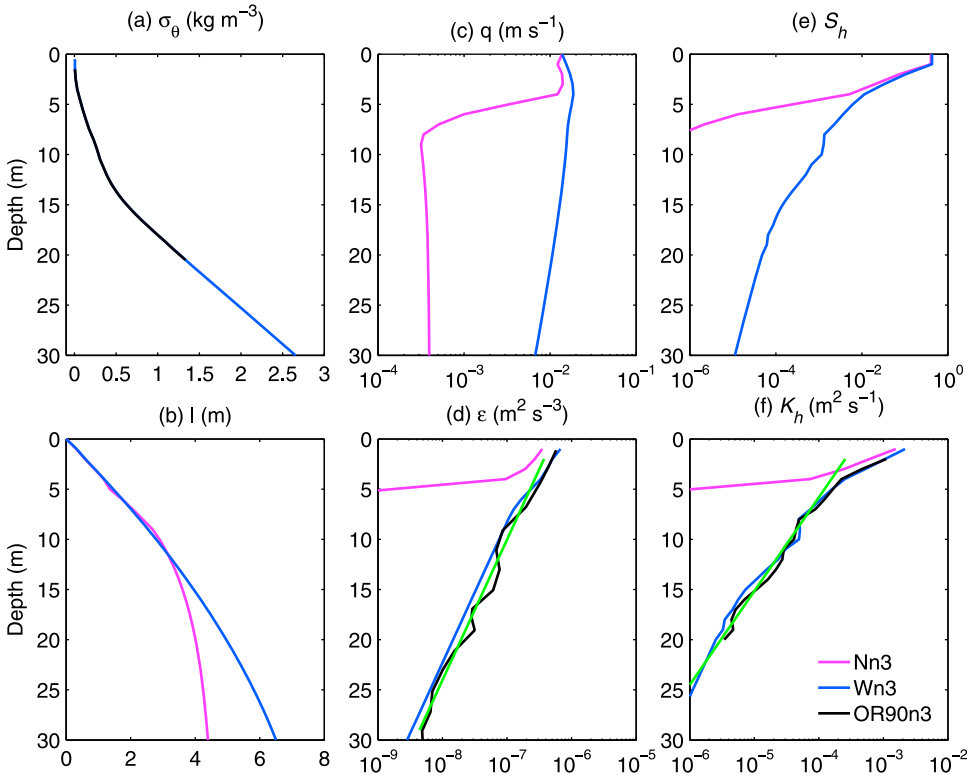

Figure 7. (a) The profiles of prescribed potential density and comparisons of simulated (b) turbulence length scale l, (c) turbulence velocity magnitude q, (d) dissipation rate ε, (e) stability factor S_h, and (f) vertical diffusivity K_h in experiments Nn3 (pink lines) and Wn3 (blue lines). The black line in Figure 7a is the observed potential density for OR90n3; the green and black lines in Figure 7d are the TKE dissipation rates defined in equation (5) and from the observation, respectively; and the green and black lines in Figure 7f are the vertical diffusivities defined in equations (11) and (12), respectively.

Richardson number. Two prognostic equations are solved for q^2 and l, in which the shear production of TKE is

$$P_S = K_m\left[\left(\frac{\partial u}{\partial z}\right)^2+\left(\frac{\partial v}{\partial z}\right)^2\right]. \tag{17}$$

The dissipation rate is calculated by

$$\varepsilon = \frac{q^3}{B_1 l}, \tag{18}$$

where u and v are the horizontal mean velocities and B_1 (= 16.6) is an empirical constant.

[25] From equation (5), the wave-turbulence interaction can transfer a large amount of energy from the wavefields to turbulence. Thus, the production of TKE of the upper ocean should include the effect of surface waves if surface waves are present [*McWilliams et al.*, 1997; *Teixeira and Belcher*, 2002; *Kantha and Clayson*, 2004; *Ardhuin and Jenkins*, 2006], then

$$P = P_S + P_w, \tag{19}$$

where P_w is the rate of TKE production due to wave-turbulence interaction, whose value should be equal to the loss of nonbreaking wave energy, i.e., ε_w in equation (5).

[26] Although wave breaking enhances TKE of the upper ocean greatly, its effect is mainly confined within the near-surface zone [*Rapp and Melville*, 1990; *Craig and Banner*, 1994; *Soloviev and Lukas*, 2003]. For example, based on the analysis of monthlong near surface turbulence data taken in the western equatorial Pacific during the TOGA Coupled Ocean-atmosphere Response Experiment (COARE), *Soloviev and Lukas* [2003] concluded that most of the wave-breaking energy is dissipated within the depth of only ~20% of significant wave height. Thus the effect of wave breaking may be less significant beyond this thin layer.

[27] We have carried out five groups of experiments corresponding to OR90, in order to examine the effects of the energy transfer induced by wave-turbulence interaction. OR90n3 is an ideal case for validating wave-turbulence interaction, in which the surface wind stress and heat flux were quite weak, and no discernible whitecaps were observed. The first group of experiments corresponding to OR90n3 includes two cases, i.e., experiments Nn3 and Wn3. For experiment Nn3, the effect of surface waves is absent, while the effect of wave-turbulence interaction is incorporated into experiment Wn3 via equation (19). In the two cases, the surface wind stress is set as 0.03 N m^{-2}, and the profiles of potential density are prescribed for that of OR90n3 and not change with the time during model integration. In addition, the profile of the observed potential density is shallower than that of the dissipation rate for OR90n3, thus we extend it downward to 35 m according to its trend (Figure 7a).

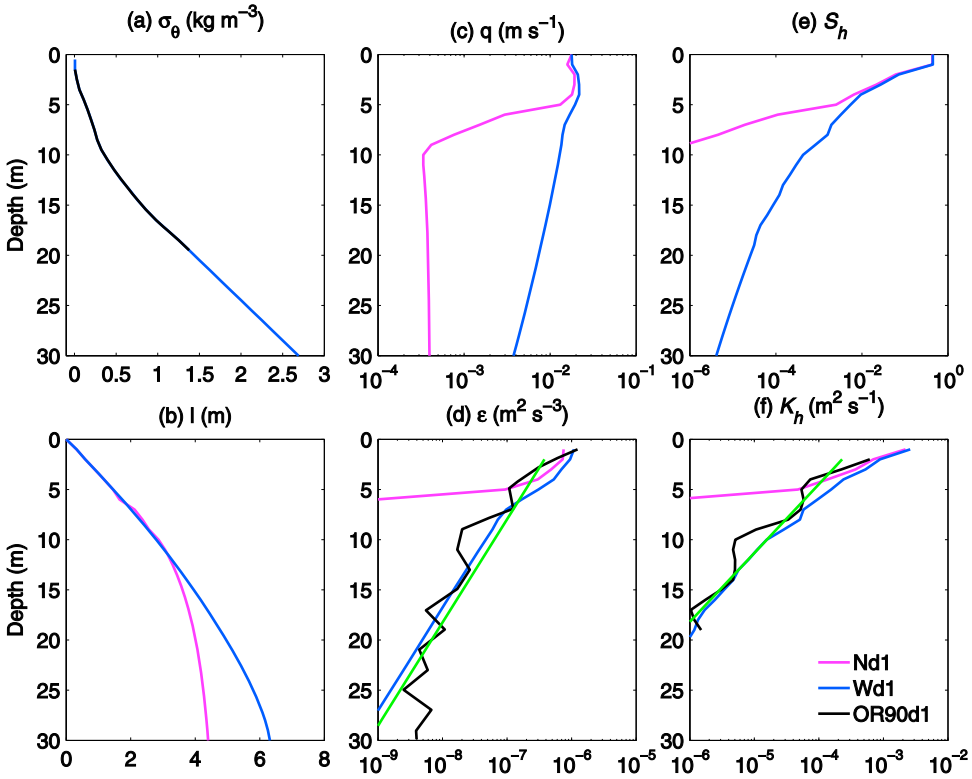

Figure 8. Same as Figure 7 but for experiments Nd1 (pink lines) and Wd1 (blue lines).

[28] Other four groups of experiments, named as Nd1/Wd1, Nd2/Wd2, Nn1/Wn1, and Nn2/Wn2, are similar to that in the first group, but corresponding to OR90d1, OR90d2, OR90n1, and OR90n2, respectively. The effect of wave breaking is not included in the model, because the whitecaps are indiscernible or occasional in most cases.

[29] For all experiments, the water depth is set as 100 m with a resolution of 1 m. The time step is 180 s, the Coriolis parameter f is set as the value at 45°N, and the background mixing is set as 10^{-6} m^2 s^{-1}. All the cases start from rest, and the model results at hour 24 are analyzed in section 5.2.

5.2. Model Results

[30] The vertical profiles of turbulence characteristics obtained by simulation of the first group of numerical experiments are shown in Figures 7b–7f. On can see that all of them are very sensitive to inclusion of wave-turbulence interaction. (The behavior of the vertical viscosity K_m and stability function S_m are not shown because of their similarity to that of K_h and S_h). In the case without considering the effect of wave-turbulence interaction, the strong turbulence velocity q is mainly confined in the near-surface zone (Figure 7c). Below the zone, q decreases rapidly down to an order of magnitude. In the Mellor-Yamada model, the dissipation rate ε, and the vertical diffusivity K_h are associated closely with q, thus the high values of the simulated ε and K_h are also confined in the near-surface zone (Figures 7d and 7f). This usually results in insufficient mixing in the upper ocean, a common problem of ocean models based on the Mellor-Yamada scheme, which usually generates too warm sea surface temperature and an overly shallow mixed layer in summer [*Martin*, 1985; *Ezer*, 2000].

[31] The simulation would be improved when the effect of wave-turbulence interaction is incorporated into the numerical model, the penetration depth of q increases greatly compared to that in absence of surface waves (Figure 7c), which improves the simulation of ε significantly (Figure 7d). On the other hand, l below about 15 m also increases in this case (Figure 7b). The changes in q and l would cause a significant increase of the stability factor S_h via changing the Richardson number defined as $G_h = -l^2N^2/q^2$ [*Ezer*, 2000]. In the Mellor-Yamada model, the vertical diffusivity K_h is proportional to q, l, and S_h. Thus the simulated K_h is much improved (Figure 7f).

[32] The other four groups of experiments are corresponding to the other four periods of observations of OR90. The simulation results exhibit a similar improvement to the first group (Figures 8–11). However, in the three groups of experiments with surface wind stress of 0.12~0.23 N m^{-2} (Figures 9–11), i.e., OR90d2, OR90n1, and OR90n2, the observed dissipation rate ε near the surface is much smaller than that predicted by the classical law of the wall. Thus the simulated ε is much larger than the observations in the upper 10~15 m, no matter whether including wave-turbulence interaction or not. In the models, the falsely large ε near the surface may be caused by too large velocity shear of the mean current.

[33] In the two groups of experiments with the weak wind stress (Figures 7 and 8), it is interesting to note that the profiles of simulated ε and K_h with wave-turbulence interaction are very close to the observations, and that defined by

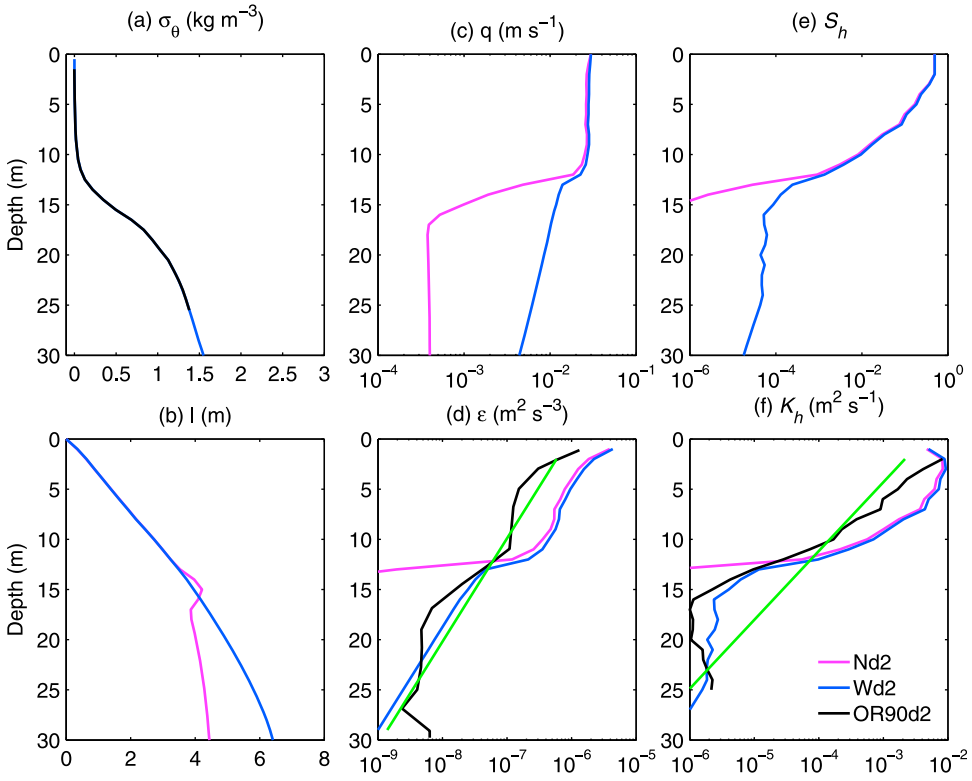

Figure 9. Same as Figure 7 but for experiments Nd2 (pink lines) and Wd2 (blue lines).

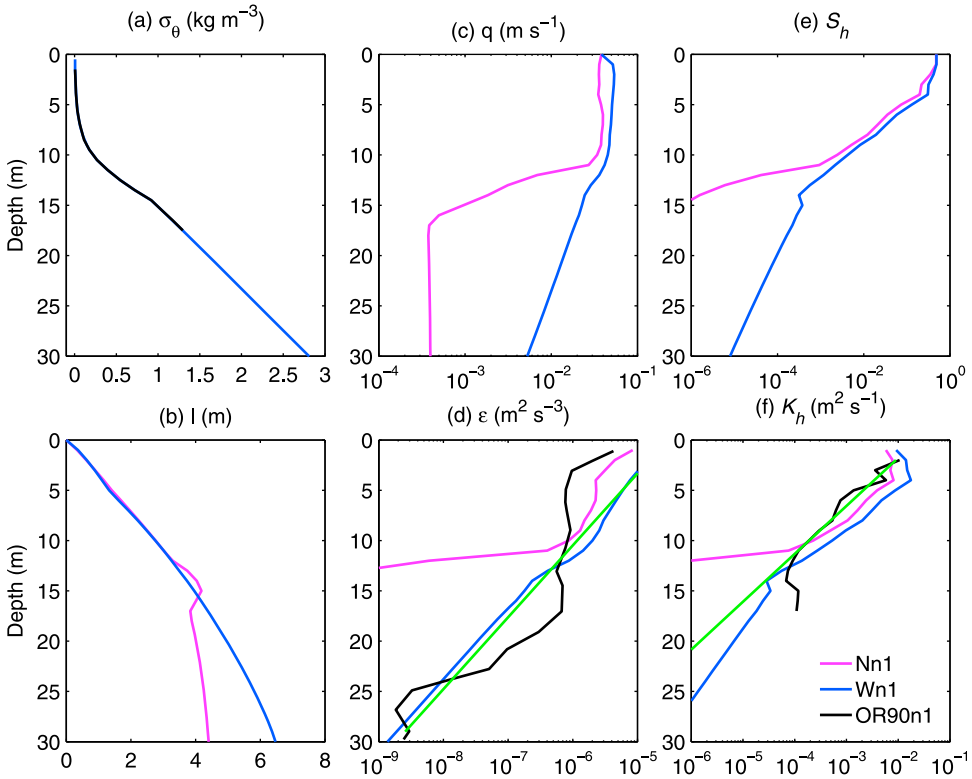

Figure 10. Same as Figure 7 but for experiments Nn1 (pink lines) and Wn1 (blue lines).

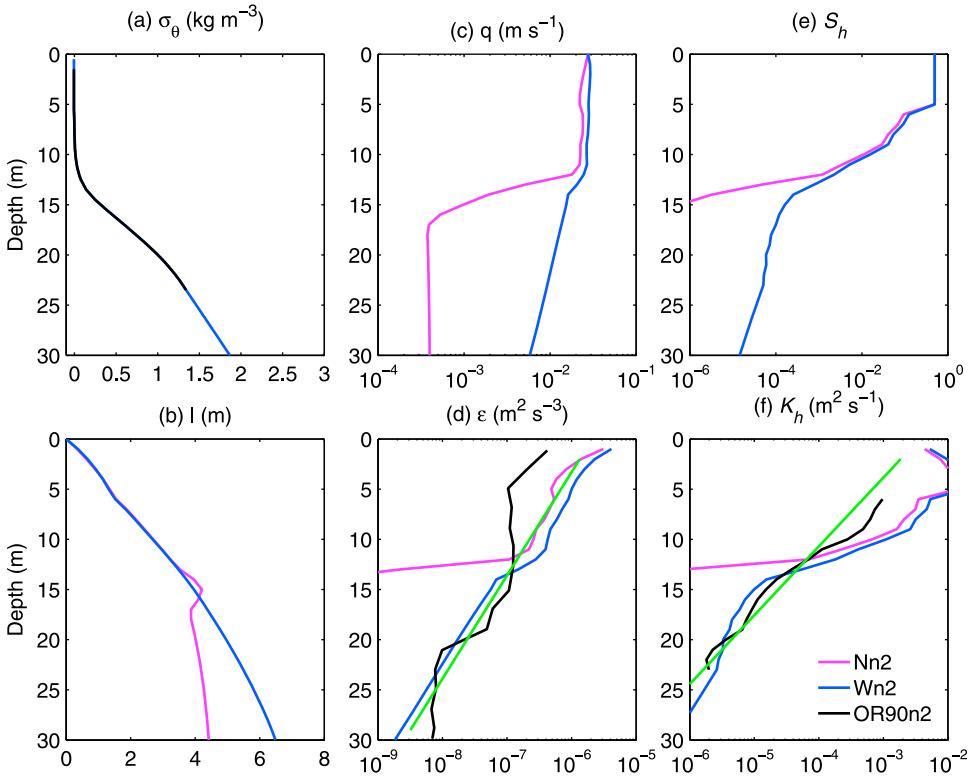

Figure 11. Same as Figure 7 but for experiments Nn2 (pink lines) and Wn2 (blue lines).

equations (5) and (11) throughout the depth. These results imply that turbulence and the vertical diffusivity in the upper ocean are controlled by wave-turbulence interaction under weak wind conditions. For moderate and strong winds, the TKE near the surface are greatly affected by wave breaking and other processes, whereas below this layer, wave-turbulence interaction associated with the swells plays an important role in regulating the turbulence owing to its deep influencing depth (Figures 9–11).

6. Conclusions

[34] The interaction among the surface waves, mean current, and turbulence in the ocean causes energy transfer from the wavefield to the turbulence, and affects the budget of the TKE in the upper ocean, then regulates the mixing process. This paper deals with the TKE dissipation rate induced by wave-turbulence interaction, and its induced mixing based on the field observations and a one-dimensional Mellor-Yamada level 2.5 turbulence closure model. The results show that the dissipation rate induced by wave-turbulence interaction is in proportion to $u_{s0}u_*^2$ and $\sqrt{\delta}/L$. This implies that the steep waves and strong wind stress result in strong wave-turbulence interaction, then produce quick dissipation in the ocean. This dissipation rate decays downward as e^{2kz} away from the surface. Thus the dissipation induced by short waves attenuates rapidly with the depth, and their effects are confined within a thin layer near the surface, while that induced by the swells may penetrate much deeper.

[35] The mixing induced by wave-turbulence interaction is also related to $u_{s0}u_*^2$ and the characteristics of surface waves, and it decays with the depth as e^{3kz}. Thus the mixing from the swells with larger wavelengths can penetrate a greater depth compared to that by waves with smaller wavelengths and wave breaking. The mixing from the swells could affect out of the mixed layer, even penetrate the seasonal thermocline in summertime.

[36] The decay of waves induced by wave-turbulence interaction is also discussed. We find that the decay time scale of the swells is in proportion to cL/u_*^2, but in inverse proportion to $\sqrt{\delta}$. This indicates that the decay rate is much weaker for the long-wavelength and smooth swells, so that they can propagate over a long distance with a little energy loss, whereas short-wavelength and steep waves are attenuated rapidly.

[37] A series of numerical experiments are performed to evaluate the effects of wave-turbulence interaction. In the cases without the surface waves, the simulated dissipation rate and vertical mixing are mainly confined in the shallow near-surface zone. Fortunately, the results from the cases with the effect of wave-turbulence interaction show significant improvements in the simulation of turbulence characteristics. The simulated profiles of the dissipation rate and mixing are very close to the observations. The numerical experiments indicate that wave-turbulence interaction is an important mechanism for regulating the turbulence and the mixing in the upper ocean, which can alleviate the problem of the insufficient mixing simulated by the classical Mellor-Yamada [*Mellor and Yamada*, 1982] model.

[38] The results of this study indicate that the wave energy dissipation induced by wave-turbulence interaction is a nonnegligible source of TKE in the upper ocean, and plays

an important role in regulating the upper ocean mixing. However, the mechanisms of wave-turbulence interaction are still far from being completely understood. Moreover the regressed parameters of parameterization are dependent on the limited observations. Therefore, further studies and observations are needed in order to gain further understanding of the roles of surface waves in the ocean dynamics and climate system.

[39] **Acknowledgments.** This paper was supported by the National Natural Science Foundation of China through grants 40806017 and 40730842. The valuable comments from two anonymous reviewers are highly appreciated.

References

Agrawal, Y. C., E. A. Terray, M. A. Donelan, P. A. Hwang, A. J. Williams III, W. M. Drennan, K. K. Kahma, and S. A. Kitaigorodskii (1992), Enhanced dissipation of kinetic energy beneath surface waves, *Nature*, *359*, 219–220, doi:10.1038/359219a0.

Anis, A., and J. N. Moum (1995), Surface wave-turbulence interactions: Scaling $\varepsilon(z)$ near the sea surface, *J. Phys. Oceanogr.*, *25*, 2025–2045, doi:10.1175/1520-0485(1995)025<2025:SWISNT>2.0.CO;2.

Ardhuin, F., and A. D. Jenkins (2006), On the interaction of surface waves and upper ocean turbulence, *J. Phys. Oceanogr.*, *36*, 551–557, doi:10.1175/JPO2862.1.

Babanin, A. V. (2006), On a wave-induced turbulence and a wave-mixed upper ocean layer, *Geophys. Res. Lett.*, *33*, L20605, doi:10.1029/2006GL027308.

Babanin, A. V., and B. K. Haus (2009), On the existence of water turbulence induced by non-breaking surface waves, *J. Phys. Oceanogr.*, *39*, 2675–2679, doi:10.1175/2009JPO4202.1.

Burchard, H. (2001), Simulating the wave-enhanced layer under breaking surface waves with two-equation turbulence models, *J. Phys. Oceanogr.*, *31*, 3133–3145, doi:10.1175/1520-0485(2001)031<3133:STWELU>2.0.CO;2.

Cheung, T. K., and R. L. Street (1988), The turbulent layer in the water at an air-water interface, *J. Fluid Mech.*, *194*, 133–151, doi:10.1017/S0022112088002927.

Craig, P. D., and M. L. Banner (1994), Modeling wave-enhanced turbulence in the ocean surface layer, *J. Phys. Oceanogr.*, *24*, 2546–2559, doi:10.1175/1520-0485(1994)024<2546:MWETIT>2.0.CO;2.

Donelan, M. A. (1998), Air-water exchange processes, in *Physical Processes in Lakes and Oceans*, *Coastal and Estuarine Stud.*, vol. 54, edited by J. Imberger, pp. 19–36, AGU, Washington, D. C.

Drennan, W. M., M. A. Donelan, E. A. Terray, and K. B. Katsaros (1996), Oceanic turbulence dissipation measurements in SWADE, *J. Phys. Oceanogr.*, *26*, 808–815, doi:10.1175/1520-0485(1996)026<0808:OTDMIS>2.0.CO;2.

Ezer, T. (2000), On the seasonal mixing layer simulated by a basin-scale ocean model and the Mellor-Yamada turbulence scheme, *J. Geophys. Res.*, *105*, 16,843–16,855, doi:10.1029/2000JC900088.

Ferrari, R., and C. Wunsch (2009), Ocean circulation kinetic energy: Reservoirs, sources, and sinks, *Annu. Rev. Fluid Mech.*, *41*, 253–282, doi:10.1146/annurev.fluid.40.111406.102139.

Gemmrich, J. R., and D. M. Farmer (2004), Near-surface turbulence in the presence of breaking waves, *J. Phys. Oceanogr.*, *34*, 1067–1086, doi:10.1175/1520-0485(2004)034<1067:NTITPO>2.0.CO;2.

Grachev, A. A., and C. W. Fairall (2001), Upward momentum transfer in the marine boundary layer, *J. Phys. Oceanogr.*, *31*, 1698–1711, doi:10.1175/1520-0485(2001)031<1698:UMTITM>2.0.CO;2.

Huang, C. J., F. Qiao, and Z. Song (2008), The effect of the wave-induced mixing on the upper ocean temperature in a climate model, *Acta Oceanol. Sin.*, *27*(3), 104–111.

Jacobs, C. A. (1978), Numerical simulations of the natural variability in water temperature during BOMEX using alternative forms of the vertical eddy exchange coefficients, *J. Phys. Oceanogr.*, *8*, 119–141, doi:10.1175/1520-0485(1978)008<0119:NSOTNV>2.0.CO;2.

Jiang, J.-Y., R. L. Street, and S. P. Klotz (1990), A study of water-turbulence interaction by use of a nonlinear water wave decomposition technique, *J. Geophys. Res.*, *95*, 16,037–16,054, doi:10.1029/JC095iC09p16037.

Kantha, L. (2006), A note on the decay rate of swell, *Ocean Modell.*, *11*, 167–173, doi:10.1016/j.ocemod.2004.12.003.

Kantha, L. H., and C. A. Clayson (2004), On the effect of surface gravity waves on mixing in the oceanic mixed layer, *Ocean Modell.*, *6*, 101–124, doi:10.1016/S1463-5003(02)00062-8.

Kantha, L., P. Wittmann, M. Sclavo, and S. Carniel (2009), A preliminary estimate of the Stokes dissipation of wave energy in the global ocean, *Geophys. Res. Lett.*, *36*, L02605, doi:10.1029/2008GL036193.

Kara, A. B., P. A. Rochford, and H. E. Hurlburt (2003), Mixed layer depth variability over the global ocean, *J. Geophys. Res.*, *108*(C3), 3079, doi:10.1029/2000JC000736.

Kinsman, B. (1965), *Wind Waves*, 676 pp., Prentice Hall, Englewood Cliffs, N. J.

Kitaigorodskii, S. A., and J. L. Lumley (1983), Wave-turbulence interaction in the upper ocean. Part I: The energy balance of the interacting fields of surface wind waves and wind-induced three-dimension turbulence, *J. Phys. Oceanogr.*, *13*, 1977–1987, doi:10.1175/1520-0485(1983)013<1977:WTIITU>2.0.CO;2.

Kitaigorodskii, S. A., M. A. Donelan, J. L. Lumley, and E. A. Terray (1983), Wave-turbulence interaction in the upper ocean. Part II: Statistical characteristics of wave and turbulence components of the random velocity field in the marine surface layer, *J. Phys. Oceanogr.*, *13*, 1988–1999, doi:10.1175/1520-0485(1983)013<1988:WTIITU>2.0.CO;2.

Kudryavtsev, V. N., and V. K. Makin (2004), Impact of swell on the marine atmospheric boundary layer, *J. Phys. Oceanogr.*, *34*, 934–949, doi:10.1175/1520-0485(2004)034<0934:IOSOTM>2.0.CO;2.

Lettvin, E. E., and J. F. Vesecky (2001), Estimation of wind friction velocity and direction at the ocean surface from physical models and space-borne radar scatterometer measurements, *J. Geophys. Res.*, *106*, 22,503–22,519, doi:10.1029/1999JC000077.

Martin, P. J. (1985), Simulation of the mixed layer at OWS November and Papa with several models, *J. Geophys. Res.*, *90*(C1), 903–916.

McWilliams, J. C., P. P. Sullivan, and C.-H. Moeng (1997), Langmuir turbulence in the ocean, *J. Fluid Mech.*, *334*, 1–33, doi:10.1017/S0022112096004375.

Mellor, G., and A. Blumberg (2004), Wave breaking and ocean surface layer thermal response, *J. Phys. Oceanogr.*, *34*, 693–698, doi:10.1175/2517.1.

Mellor, G., and T. Yamada (1982), Development of a turbulence closure model for geophysical fluid problems, *Rev. Geophys.*, *20*, 851–875, doi:10.1029/RG020i004p00851.

Osborn, T. R. (1980), Estimates of the local rate of vertical diffusion from dissipation measurements, *J. Phys. Oceanogr.*, *10*, 83–89, doi:10.1175/1520-0485(1980)010<0083:EOTLRO>2.0.CO;2.

Osborn, T., D. M. Farmer, S. Vagle, S. A. Thorpe, and M. Cure (1992), Measurements of bubble plumes and turbulence from a submarine, *Atmos. Ocean*, *30*, 419–440.

Phillips, O. M. (1961), A note on the turbulence generated by gravity waves, *J. Geophys. Res.*, *66*, 2889–2893, doi:10.1029/JZ066i009p02889.

Plueddemann, A. J., J. A. Smith, D. M. Farmer, R. A. Weller, W. R. Crawford, R. Pinkel, S. Vagle, and A. Gnanadesikan (1996), Structure and variability of Langmuir circulation during the Surface Waves Processes Program, *J. Geophys. Res.*, *101*, 3525–3543, doi:10.1029/95JC03282.

Qiao, F., Y. Yuan, Y. Yang, Q. Zheng, C. Xia, and J. Ma (2004), Wave-induced mixing in the upper ocean: Distribution and application to a global ocean circulation model, *Geophys. Res. Lett.*, *31*, L11303, doi:10.1029/2004GL019824.

Rapp, R. J., and W. K. Melville (1990), Laboratory measurements of deep-water breaking waves, *Philos. Trans. R. Soc. London, Ser. B*, *A331*, 735–800.

Rascle, N., F. Ardhuin, P. Queffeulou, and D. Croizé-Fillon (2008), A global wave parameter database for geophysical applications. Part 1: Wave-current-turbulence interaction parameters for the open ocean based on traditional parameterizations, *Ocean Modell.*, *25*, 154–171, doi:10.1016/j.ocemod.2008.07.006.

Soloviev, A., and R. Lukas (2003), Observation of wave-enhanced turbulence in the near-surface layer of the ocean during TOGA COARE, *Deep Sea Res., Part I*, *50*, 371–395, doi:10.1016/S0967-0637(03)00004-9.

Song, Z., F. Qiao, Y. Yang, and Y. Yuan (2007), An improvement of the too cold tongue in the tropical Pacific with the development of an ocean-wave-atmosphere coupled numerical model, *Prog. Nat. Sci.*, *17*(5), 576–583, doi:10.1080/10020070708541038.

Teixeira, M. A. C., and S. E. Belcher (2002), On the distortion of turbulence by a progressive surface wave, *J. Fluid Mech.*, *458*, 229–267, doi:10.1017/S0022112002007838.

Teng, Y., Y. Yang, F. Qiao, J. Lu, and X. Yin (2009), Energy budget of surface waves in the global ocean, *Acta Oceanol. Sin.*, *28*(3), 5–10.

Terray, E. A., M. A. Donelan, Y. C. Agrawal, W. M. Drennan, K. K. Kahma, A. J. Williams III, P. A. Hwang, and S. A. Kitaigorodskii (1996), Estimates of kinetic dissipation under breaking waves, *J. Phys. Oceanogr.*, *26*, 792–807, doi:10.1175/1520-0485(1996)026<0792:EOKEDU>2.0.CO;2.

Thais, L., and J. Magnaudet (1996), Turbulent structure beneath surface gravity waves sheared by the wind, *J. Fluid Mech.*, *328*, 313–344, doi:10.1017/S0022112096008749.

Veron, F., W. K. Melville, and L. Lenain (2009), Measurements of ocean surface turbulence and wave-turbulence interactions, *J. Phys. Oceanogr.*, *39*, 2310–2323, doi:10.1175/2009JPO4019.1.

Wang, W., and R. X. Huang (2004), Wind energy input to the surface waves, *J. Phys. Oceanogr.*, *34*, 1276–1280, doi:10.1175/1520-0485(2004)034<1276:WEITTS>2.0.CO;2.

Wüest, A., G. Piepke, and D. C. Van Senden (2000), Turbulence kinetic energy balance as a tool for estimating vertical diffusivity in wind-forced stratified waters, *Limnol. Oceanogr.*, *45*(6), 1388–1400.

Xia, C., F. Qiao, Y. Yang, J. Ma, and Y. Yuan (2006), Three-dimensional structure of the summertime circulation in the Yellow Sea from a wave-tide-circulation model, *J. Geophys. Res.*, *111*, C11S03, doi:10.1029/2005JC003218.

Young, I. R., and A. V. Babanin (2006), Spectral distribution of energy dissipation of wind-generated waves due to dominant wave breaking, *J. Phys. Oceanogr.*, *36*, 376–394, doi:10.1175/JPO2859.1.

Zhang, S. W., Y. L. Yuan, and Q. A. Zheng (2007), Modeling of the eddy viscosity by breaking waves, *Acta Oceanol. Sin.*, *26*(6), 116–123.

C. J. Huang and F. Qiao, Key Laboratory of Marine Science and Numerical Modeling, First Institute of Oceanography, State Oceanic Administration, 6 Xianxialing Road, Qingdao 266061, China. (qiaofl@fio.org.cn)